Received: 28 August 2018 | Revised: 4 December 2018 | Accepted: 6 December 2018

DOI: 10.1002/jcla.22843

RESEARCH ARTICLE

WILEY

Upregulation of miR-146a-5p is associated with increased proliferation and migration of vascular smooth muscle cells in aortic dissection

Ling Xue | Songyuan Luo | Huanyu Ding | Yuan Liu | Wenhui Huang | Xiaoping Fan | Min Wu | Xuhua Jian | Cheng Huang | Jianfang Luo | Ruixin Fan

Guangdong Cardiovascular Institute, Guangdong Provincial People' Hospital, Guangdong Academy of Medical Sciences, Guangdong, Guangzhou, China

Correspondence
Ruixin Fan, Jianfang Luo and Cheng Huang, Guangdong Cardiovascular Institute, Guangdong, Guangzhou, China.
Emails: syfanruixin@sina.com; jianfangluo@sina.com; linfeng7822@sina.com

Funding information
the National Natural Science Foundation, Grant/Award Number: 81300230 and 81470571; the Guangzhou City Science and Technology Programme, Grant/Award Number: 201508020114; the Guangdong Province Science and Technology Programme, Grant/Award Number: 2014A020215023; the Science and Technology Planning Project, Grant/Award Number: 201300000180; the National Key R&D Program of China, Grant/Award Number: 2017YFC130800

Background: This study aimed to investigate whether miR-146a-5p was involved in the pathogenesis of thoracic aortic dissection (AD) via regulating the biological function of vascular smooth muscle cells (VSMCs).

Methods: Circulating miR-146a-5p level was measured by quantitative polymerase chain reaction (qPCR) in AD patients and healthy controls. Human dissected aortic samples were obtained from patients with thoracic AD Stanford type A undergoing surgical repair, and normal control samples were from organ donors who died from nonvascular diseases. The expression level of miR-146a-5p was detected using qPCR in each sample. The expression of SMAD4, which is involved in the TGF-β pathway and indicated as the target gene of miR-146a-5p, was measured by qPCR and Western blot analysis at the mRNA level and protein level, respectively. Subsequently, VSMCs were transfected with miR-146a-5p mimics or inhibitors in vitro. VSMC proliferation and migration were detected using 3-(4,5-dimethylthiazol-2-yl)-2,5-diphenyltetrazolium bromide and Transwell assay, respectively. Flow cytometry was used to identify apoptosis. The expression of SMAD4 in VSMCs was determined using qPCR and Western blot analysis.

Results: Plasma level of miR-146a-5p is significantly higher in the AD group as compared with the control group. The expression of miR-146a-5p was significantly upregulated in dissected aorta compared with controls ($P < 0.05$). The overexpression of miR-146a-5p significantly induced VSMC proliferation and migration in vitro.

Conclusions: The expression of SMAD4 was modulated by miR-146a-5p. miR-146a-5p induced VSMC proliferation and migration through targeting SMAD4 and hence might be potentially involved in the development of AD.

KEYWORDS
aortic dissection, migration, miR-146a-5p, proliferation, SMAD4, vascular smooth muscle cell

1 | INTRODUCTION

Aortic dissection (AD), as one of the highly lethal vascular diseases, cannot be reliably prevented pharmacologically thus far because the molecular mechanism of AD is poorly understood and hence dissection, progression, and rupture. Therefore, it is pivotal to further explore the mechanisms of AD.[1] As the major cells in aortic media layer, VSMCs have been taken as playing a key role in maintaining homeostasis of the aortic wall.[2-4] Of note, dysfunction of proliferation and migration in VSMCs has been reported to be involved in the development of vascular diseases.[5,6]

MicroRNA is a class of evolutionarily conserved, noncoding small RNAs that negatively regulate the expression of protein-coding gene transcripts. Previous studies revealed the involvement ofmiR146a-5p in modulating immune system and in myeloid tumorigenesis.[7] Further, bioinformatics indicated that miR146a-5p participated in cell proliferation and migration.[8] Thus, considerable attention has been attracted to the role of miR146a-5p in vascular diseases. However, the causal relationship between miR146a-5p and AD has never been reported.

In this study, the upregulation of miR146a-5p in aortic specimens of AD was confirmed. It revealed the effects of miR146a-5p on VSMCs function. Further, in vitro data indicated that the expression of SMAD4, a member of TGF-β family, was regulated by miR146a-5p. Further, circulating miR-146a-5p is significantly higher in the AD group compared to the control group. Taken together, the results shed new light on the involvement of miRNAs in the molecular regulation of VSMC function and AD.

2 | MATERIALS AND METHODS

2.1 | Participants' recruitment and sample collection

Plasma samples were obtained from 43 patients with AD Stanford type A and 36 healthy controls, respectively. Whole venous blood (5-10 mL) was extracted from elbow vein after 12- to 14-hours fasting and then centrifuged at 3000 rpm for 10 minutes under room temperature. After phase separation, plasma was collected and stored at −80°C until use. Aortic samples were acquired from nine patients with AD Stanford type A who underwent surgical aortic repair (Table S1). Patients with Marfan syndrome, Ehlers-Danlos syndrome, Loeys-Dietz syndrome, Turner syndrome, congenital bi-leaflet aortic valves, aortic aneurysm, traumatic dissection, and other connective tissue disorders, or those aged <18 years were excluded. Control aortic samples were collected from eight donors who died from nonvascular diseases (Table S1). The aortic sample was rapidly collected within 30 minutes after excision. All specimens were rinsed at least five times in precooled saline; then, the thrombus and adventitia were removed immediately using eye scissors and sterile tweezers on a clean Petri dish, and then, tissue samples were sliced into approximately 2-mm sections and placed in sterile Eppendorf (EP) tubes, followed by stored at liquid nitrogen for use. The entire procedure was performed within 10 minutes. No additional operation was performed beyond the standard procedure to obtain above samples. The demographic and clinical characteristics of participants are presented in Table 1.

The present study has been approved by the Medical Ethics Committee of Guangdong General Hospital and conducted complying with the Declaration of Helsinki. Written informed consents were obtained from each participant before inclusion.

2.2 | RNA isolation and quantitative reverse transcription-polymerase chain reaction (RT-PCR)

Total RNA containing small RNAs was extracted from aorta tissue or cultured VSMCs using the TRIzol reagent (Invitrogen, Carlsbad, CA, USA), then reversely transcribed into complementary DNA (cDNA) using a Geneseed II First Strand cDNA Synthesis Kit (Geneseed Biotech Co., Ltd. Guangdong, China) according to the manufacturer's protocols.[9] A PrimeScript Reverse Transcription (RT) Reagent Kit (TaKaRa, Tokyo, Japan) was used to synthesize cDNA with 500 ng of total RNA. Subsequently, quantitative PCR was performed using the Geneseed Quantitative Polymerase Chain Reaction (qPCR) SYBR Green Master Mix (Geneseed Biotech Co., Ltd.) in ABI 7500 machine (ABI, Waltham, MA, USA) according to the manufacturer's protocol. According to gene sequences published in GenBank, primers shown in Table 2 were constructed using Primer 5.0 software (Molecular Biology Insights, Colorado Springs, CO, USA) and checked by Oligo 7 and NCBI BLAST. Negative controls (without template) were included in each step. Each SYBR Green reaction mixture (total volume, 20 μL) contained 2 μL of cDNA as template and 10 μmol/L of each primer. The RT reaction was conducted at 25°C for 10 minutes, subsequently 42°C for 15 minutes and 85°C for 5 minutes. PCR mixture was incubated at 95°C for 5 minutes, then 40 cycles at 95°C for 10 seconds, 60°C for 34 seconds, and 60°C for 60 seconds, respectively. After the final cycle of qRT-PCR, the samples were taken to the heat dissociation protocol to check for the presence of the only peak to identify the only one qRT-PCR product detected by SYBR Green dye. With β-actin as internal control, the reliability of qRT-PCR was assessed using the melting curve. The ΔCq was obtained, and the relative miR expression level was determined using

TABLE 1 Demographic and clinical characteristics of the included patients and controls

Variables	Patients (n = 9)	Controls (n = 8)	*P* value
Age, years	**51.7**	**36.5**	**0.023**
Sex, male, n (%)	9 (100%)	6 (75%)	0.832
Hypertension, n (%)	6 (70%)	2 (25%)	0.155
Hyperlipidemia, n (%)	3 (33%)	0 (0%)	0.289
Diabetes mellitus, n (%)	1 (10%)	2 (25%)	0.832
Smoking, n (%)	7 (77%)	6 (75%)	1.000
Family history of Marfan syndrome	0	0	1.00
AST (U/L)	36.5	41.8	0.248
ALT (U/L)	51.9	50.88	0.068
Cr (mmol/L)	96.5	67.3	0.056

Bold values indicate significance $P < 0.05$

TABLE 2 Sequence of primers in this study

	Sequence (5′ to 3′)
SMAD4	Forward GTGTTGATGACCTTCGTCGC
SMAD4	Reverse GGGCCCGGTGTAAGTGAAT
miR146a-5p	F-1 ATGGTTCGTGGGTGAGAACTGAATTCCATGGG
miR146a-5p	RT-1 GTCGTATCCAGTGCAGGGTCCGAGGTATTCG CACTGGATACGACCAATTCCAGGG
	Com R GTGCAGGGTCCGAGGT

the formula $2^{-\Delta Cq}$. Mean Cq values and deviations between the duplicates were computed for all samples.

2.3 | Western immunoblotting

Total protein was extracted from 100 mg aortic specimen with 1000 mL of RIPA buffer. VSMCs were washed thricely with phosphate-buffered saline and 100 μL of RIPA buffer (Cell Signaling Technology, Danvers, MA, USA) per well (six-well plate). Cells were mixed, lysed using a cell lifter (Coring Costar, Corning, NY, USA), and then transferred to EP tubes. All of the samples were normalized to 1.0 mg/mL. A total of 20 mL was loaded on a 6%-12% sodium dodecyl sulfate-polyacrylamide gel electrophoresis plate and subsequently transferred onto a polyvinylidene difluoride membrane. For one Western blot gel, the total amount of each sample was 20 μg. The membranes were blocked using 5% nonfat milk (Becton Dickinson, Franklin Lakes, NJ, USA), then washed, and probed with the following primary antibodies: rat antihuman SMAD4 (1:1000; Abcam, Cambridge, UK) and GAPDH (1:500; Abcam). Then, the membranes were incubated with a horseradish peroxidase-conjugated goat anti-rat antibody (1:2000; Sigma, Guangzhou, China) for 1 hour. Subsequently, the membranes were washed and developed using an enhanced chemiluminescence kit according to the manufacturer's protocols (Thermo Fisher, Waltham, MA, USA). Western blot assays were repeated three times. The blots were scanned using a flatbed scanner, followed by determining intensities using the Image-Pro Plus software version 6.0 (Media Cybernetics, Inc, Rockville, MD, USA).

2.4 | Luciferase assay

The 3′-untranslated region (UTR) sequence of SMAD4 gene containing miR146a-5p-binding sites was amplified using PCR. The 3′-UTR sequence was cloned into the pMIR-REPORT luciferase vector named psiCHECK2-SMAD4-wild-type. The mutation of the binding site in 3′-UTR of SMAD4 was amplified using PCR and cloned into the plasmid named psiCHECK2-SMAD4-mutant. miR146a-5p mimics and luciferase plasmid psiCHECK2-SMAD4 (wild-type/mutant, wt/mut) were transfected into 293T cells using Lipofectamine 2000 (Invitrogen; Thermo Fisher Scientific, Inc) according to the manufacturer's protocol. After cultivation for 48 hours, the cells were reaped and lysed. Luciferase activity in the cell lysates was determined using a TransDetect Double-Luciferase Reporter Assay Kit (TransGen Biotech, Beijing, China). Firefly luciferase activity was standardized to Renilla luciferase activity. The experiments were performed in triplicate.

2.5 | Cell culture and transfection

Primary human arterial smooth muscle cells (HASMCs) from human aorta were purchased from Geneseed Biotech Company and maintained in smooth muscle cell medium (Cat. No. 1101) from ScienCell supplemented with 10% fetal bovine serum, 100 μg/mL streptomycin, and 100 units/mL penicillin (all from Invitrogen) at 37°C in 5% CO_2 humidified atmosphere. All procedures were performed with cells in the third-to-sixth passages. For cell transfection, miR146a-5p mimics or inhibitors were obtained from Geneseed Biotech Company, and the transfection into HASMCs was conducted using Lipofectamine 2000 (Invitrogen) according to the manufacturer's protocols.

2.6 | Transwell HASMC migration assays

Human arterial smooth muscle cells were seeded into a 24-well plate with density of 2×10^4/well, incubated overnight, and then transfected with miR146a-5p mimics or inhibitors using Lipofectamine 2000 (Invitrogen) according to the manufacturer's protocol for 24 hours. Then, the cells were detached using 2.5% trypsin and resuspended in a serum-free medium at a concentration of 1×10^6/mL; 200 μL of cell solution was added into each upper chamber of the Transwell, and 600 μL of growth medium was added into each lower chamber. Then, the Transwell chambers were incubated at 37°C for 48 hours. The Transwell filter had 8.0-μm pores, and for the migration assay, the filter was precoated with 50 μL of Matrigel (BD Biosciences, San Jose, CA, USA). The cells remaining on the top surface of the filter were removed using a cotton swab, whereas the cells migrated to the lower surface were fixed with 10% formalin, stained with 0.5% crystal violet solution, and then counted for five random fields (×200) under a light microscope.

2.7 | Cell proliferation assay

Cell proliferation was examined using cell counting kit-8 (Dojindo, Japan) according to the manufacturer's protocols. VSMCs were seeded in 96-well plates with density of 5×10^3 cells per well. After adhesion, VSMCs were incubated in 1% fetal bovine serum (FBS) M199 media for 24 hours, followed by treatment with adenovirus at multiple infection of MOI 120 with 15% FBS M199, and the medium was displaced every 24 hours. Subsequently, 10 mL of cell counting kit-8 reagent was titrated to each well 0, 12, 24, 36, and 48 hours after transfection, and the cells were further incubated for 4 hours at 37°C. The absorbance at 450 nm was read using a spectrophotometric plate reader. VSMCs that taken as negative controls were transfected with adenovirus without the miR146a-5p interfering effect.

2.8 | HASMC viability 3-(4,5-dimethylthiazol-2-yl)-2,5-diphenyltetrazolium bromide assay

Human arterial smooth muscle cells were seeded in 96-well plates at a density of 5×10^4 cells/well, grown overnight, and then transfected with miR146a-5p mimics or inhibitors using Lipofectamine

2000 (Invitrogen) according to the manufacturer's protocols for 24 hours. The growth medium was refreshed, and the cells were cultured for the scheduled time points (24, 48, and 72 hours). At the end of each experiment, 3-(4,5-dimethylthiazol-2-yl)-2,5-diphenyltetrazolium bromide (MTT; Beyotime, Beijing, China) was added to the cell culture according to the manufacturer's protocols. The cells were further cultured for 4 hours, and then, the cell culture medium was substituted with 150 μL of dimethyl sulfoxide (DMSO). After mixing well, the absorbance at 490 nm was determined using a microplate reader (Bio-Rad 680, Hercules, CA, USA). The cell growth curve was plotted using the cell absorbance data. The experiment was performed in triplicate and repeated at least thrice.

2.9 | Apoptosis assay using flow cytometry

Human arterial smooth muscle cells were detached using 2.5% trypsin, stained with FITC-conjugated Annexin V and propidium iodide using an Annexin V-FITC Apoptosis Detection Kit (KeyGen, Jiangsu, China), and then analyzed using FACScan flow cytometry (BD Biosciences). The experiments were repeated at least three times. The apoptotic rate was quantified using the CellQuest software (BD Biosciences).

2.10 | Statistical analysis

All experimental data were expressed as mean ± standard deviation (SD) and analyzed using the Statistical Package for the Social Sciences (SPSS) 17.0 software (SPSS Inc, Chicago, IL, USA). The Kolmogorov-Smirnov test was applied to determine the normal distribution. Inter-group comparison was performed using the independent samples t test. For continuous numeric parameters with normal distribution, one-way analysis of variance was conducted to identify differences between groups. The Tukey's test was used for post hoc analyses. Significance was set at $P < 0.05$.

3 | RESULTS

3.1 | Differential expression of miR146a-5p and SMAD4 in dissected vs normal aortic tissue specimens

The Western blot analysis was performed to detect the expression level of SMAD4 protein in the human aorta. As shown in Figure 1A,B, SMAD4 was significantly downregulated in AD samples compared with NA samples. qRT-PCR was used to detect the expression of miR146a-5p and SMAD4 mRNA in AD and their matched NA samples so as to further reveal the expression of miR146a-5p (Figure 1C,D) and SMAD4 in the human aorta. The expression of miR146a-5p was significantly upregulated, whereas the expression of SMAD4 markedly decreased in the AD group. All these results suggest that SMAD4 demonstrated a downregulation character in AD samples compared with NA samples, as opposed to miR146a-5p.

3.2 | Overexpressed miR146a-5p increased HASMC proliferation and migration

Human arterial smooth muscle cells were transfected with miR146a-5p mimics or inhibitors to investigate whether miR146a-5p had a role in the regulation of biological functions of VSMCs (Figure S1). As determined by the cell viability MTT assay, the upregulation of miR146a-5p in HASMCs caused a evident increase in the number of proliferating cells, whereas the downregulation of miR146a-5p significantly decreased HASMC proliferation (Figure 2A). The

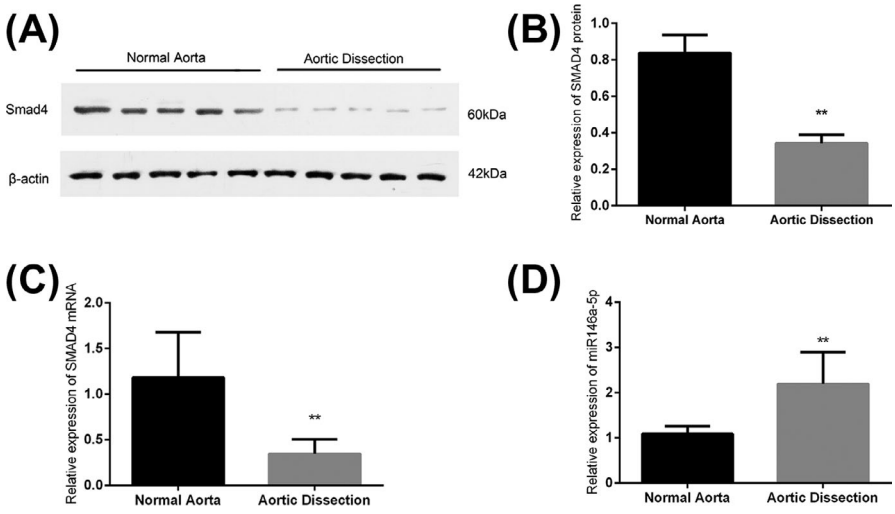

FIGURE 1 Expression of SMAD4 and miR146a-5p in human aorta samples with NA and AD, respectively. A and B, Western blot analysis for SMAD4 protein expression in human aorta samples (n = 5 per group). SMAD4 protein expression was significantly downregulated in AD samples ($P < 0.01$). C, qPCR for SMAD4 mRNA expression in human aorta samples (n = 9 for the AD group and 8 for the NA group). SMAD4 mRNA expression was significantly downregulated in AD samples ($P < 0.01$). D, qPCR for miR146a-5p expression in human aorta samples (n = 9 for the AD group and 8 for the NA group). The expression of miR146a-5p was significantly upregulated in AD samples ($P < 0.05$).

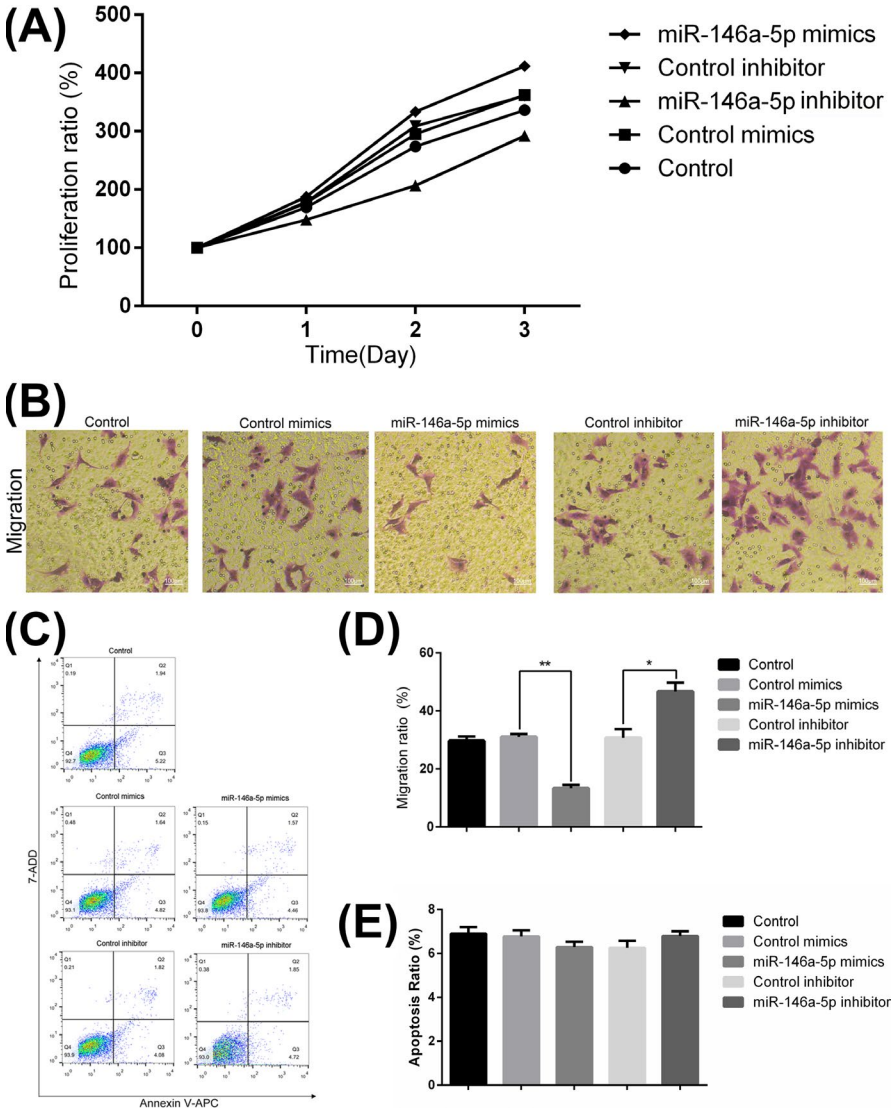

FIGURE 2 In vitro transfection of miR146a-5p mimics or inhibitors strongly altered HASMC proliferation and migration. A, Proliferation curves of HASMCs transfected with control, miR-146a-5p mimics, mimics control, inhibitors, and inhibitors control. The result showed that the proliferation ability of HASMCs was significantly inhibited 72 h after the treatment with miR-146a-5p inhibitors. On the contrary, miR146a-5p mimics improved the proliferation ability of HASMCs compared with miR-146a-5p inhibitors control (n = 5 per group). B, Results of the Transwell test showed decreased migration ability in the miR-146a-5p inhibitor group, but it significantly improved in the miR-146a-5p mimics group. Quantified data were presented as the number of migrating cells per high-power field (n = 5 per group). C, The flow cytometric analysis showed that the transfection of miR146a-5p mimics or inhibitors had no effect on HASMC apoptosis (n = 5 per group). D and E, Data were represented as mean ± SD. All the experiments were performed thrice

Transwell test was performed to identify the role of miR146a-5p in HASMC migration. Treatment with miR146a-5p mimics substantially promoted the migration response in cultured HASMCs. In contrast, the downregulation of miR146a-5p had no effect on migration (Figure 2B,D). Furthermore, a flow cytometry test was performed to evaluate the effect of miR146a-5p on HASMC apoptosis. No significant change in the apoptosis of HASMCs was observed after transfection with miR146a-5p mimics (Figure 2C,E). These in vitro observations revealed that miR146a-5p participated in HASMC proliferation and migration.

3.3 | Expression of SMAD4 was regulated by miR146a-5p

TargetScan and miRanda were used to analyze the predicted targets of miR146a-5p so as to explore the underlying effects of miR146a-5p on HASMC migration and proliferation. The study found that one target gene for miR146a-5p was SMAD4. One putative binding site was found at 390-397, which was highly conserved across species, as shown in Figure 3A, and therefore, the wild-type or mutant 3'-UTR of SMAD4 was cloned into a luciferase vector.

The luciferase reporter assay was used to confirm the predictions. The wild-type (WT) 3′-UTR and the mutated-type (Mut) 3′UTR of SMAD4 luciferase reporter vectors were constructed. 293T cells were co-transfected with miR146a-5p mimics and WT or Mut luciferase reporter vector. The relative luciferase activity significantly reduced in 293T cells co-transfected with miR146a-5p mimics and WT luciferase vector (Figure 3B). The activity of Mut luciferase reporter activity was not affected by miR146a-5p mimics in 293T cells. Therefore, miR146a-5p directly bound to 3′-UTR of SMAD4.

miR146a-5p mimics and inhibitors were transfected into HASMCs to further confirm whether SMAD4 was directly regulated by miR146a-5p. The expression of SMAD4 mRNA and protein was detected using qPCR (Figure 4A) and Western blot analysis (Figure 4B,C), respectively. The results demonstrated that the expression of SMAD4 was reduced with miR146a-5p overexpression in HASMCs, whereas miR146a-5p inhibitor increased SMAD4 mRNA and protein expression in HASMCs.

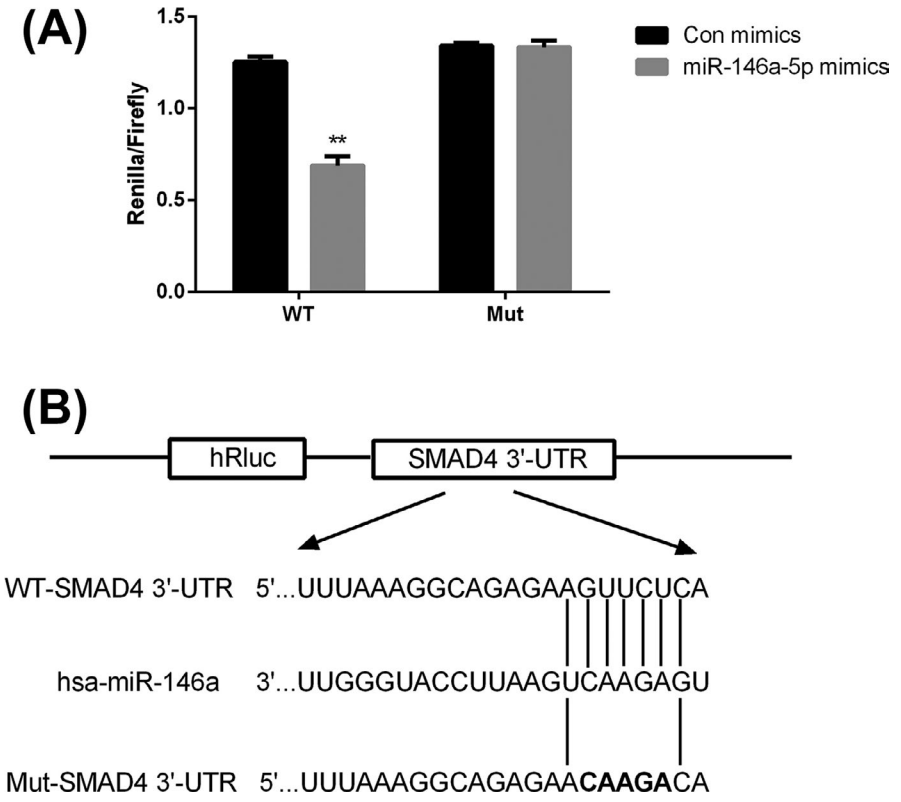

FIGURE 3 SMAD4 was a direct target of miR146a-5p. A, Sequence alignment of miR146a-5p with 3′-UTR of SMAD4 predicted using TargetScan. B, Luciferase assay results for 293T cells showed that miR146a-5p upregulation decreased luciferase activity

3.4 | Circulating miR-146a-5p level was elevated in the AD group

Forty AD patients and 36 healthy controls included for circulating miR-146a level determination showed no significant difference in age, gender, incidence of coronary artery diseases, incidence of diabetes, family history, and liver and renal functions between two groups ($P > 0.05$) (Table S2), whereas incidence of hypertension and smoking rate were significantly higher in the AD group (93.02% vs 13.89 $P < 0.05$, and 34.88% vs 8.33% $P < 0.05$, respectively). As expected, the level of circulating miRNA-146a-5p was significantly higher in AD patients as compared with that in normal controls (Figure 5).

4 | DISCUSSION

The involvement of miRNAs in aortic diseases has been reported in recent years.[10-13] A previous study profiled dysregulated miRNA expression in AD and found the expression of miR146a-5p to be upregulated.[14] Dysfunction of the miR-146 family has often been linked to inflammation and malignancies.[7] However, no published study exists about the role of miR146a-5p in the pathogenesis. The present study was performed to confirm the expression pattern of miR146a-5p in AD and its regulatory role in the biological functions of VSMC's. The study showed that miR146a-5p was significantly upregulated in AD tissues. Subsequently, the role of miR146a-5p in VSMC proliferation, migration, and apoptosis was explored. The result showed that miR146a-5p overexpression increased VSMC proliferation and migration, whereas the deletion of miR146a-5p with a specific inhibitor decreased VSMC migration and proliferation. Finally, the level of circulating miRNA-146a-5p was significantly higher in AD patients as compared with healthy controls, further corroborating the association of miR146a-5p with AD and implying miR146a-5p as a potential candidate for biomarker of AD.

Previous investigations have revealed a critical role of VSMCs in aortic walldegeneration, which has been identified as the initiation of pathologic remodeling in AD.[9,15,16] Remarkably, abnormal proliferation and migration of VSMCs have been considered potentially as the main cause of pathological vascular remodeling and vascular disease through undermining the vasculature stability.[17] Of note, Müller et al and Wang et al observed that VSMCs from dissected aorta proliferated more rapidly than VSMCs from normal aorta tissues, and the genes participate in proliferation exhibited an increased expression.[18,19] Similar to in vitro data, VSMCs overexpressing miR146a-5p showed enhanced proliferation and migration, indicating a potential involvement for miR146a-5p in the AD pathogenesis.

Further, this study identified SMAD4 as a novel target of miR146a-5p in VSMCs. SMAD4 belongs to the SMAD/TGF-β family, the members of which regulate many key cellular processes such as migration, adhesion, cell division, differentiation, and tissue homeostasis and embryogenesis in a context- and cell type-dependent manner. Zhang et al[20] indicated that SMAD4 inhibited cell locomotion by suppressing the JNK activity in human pancreatic carcinoma cells. Zong et al[21] demonstrated regulation of proliferation and invasion in ovarian carcinoma cells by miR-205 via depressing PTEN/SMAD4 expression. Moreover, the pathological SMAD4/TGF-β

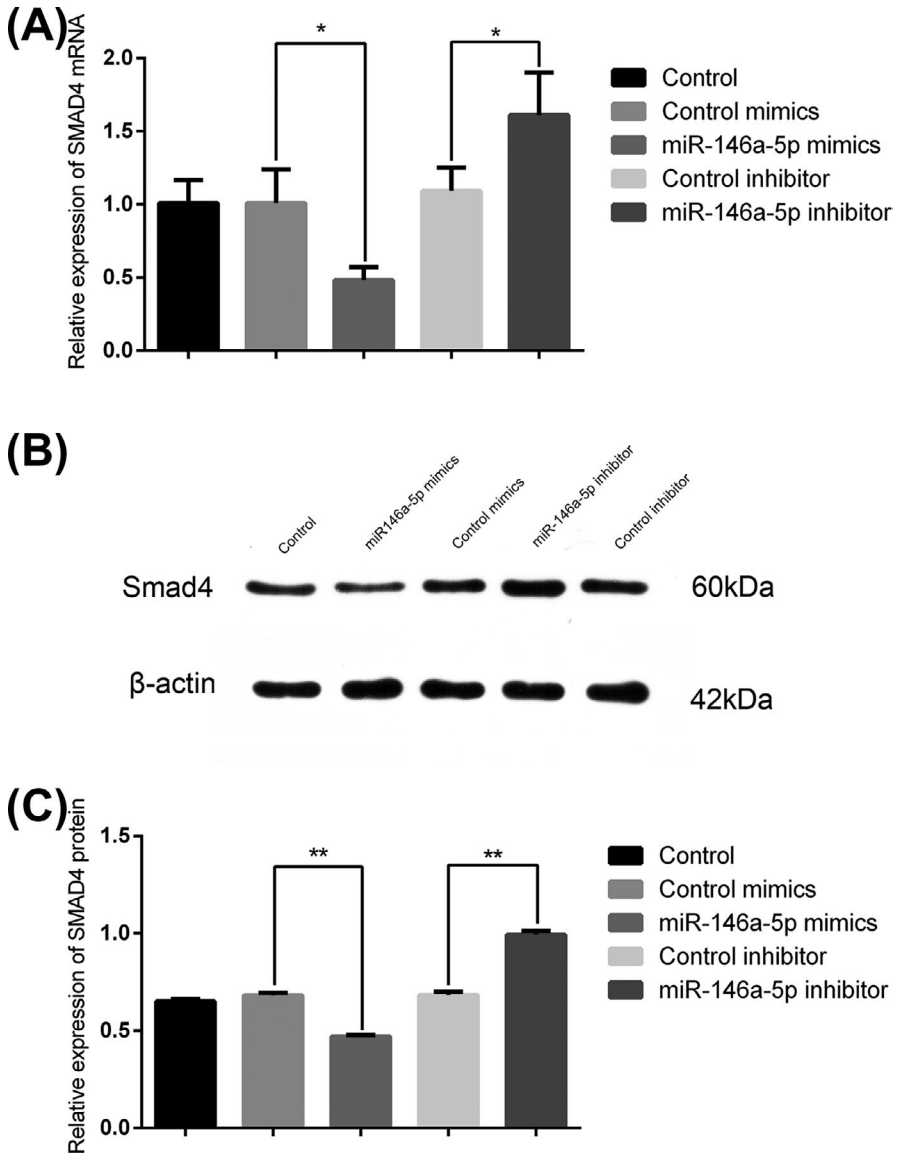

FIGURE 4 miR146a-5p suppressed the expression of SMAD4 in HASMCs. qPCR (A) and Western blot analysis (B and C) confirmed that miR146a-5p overexpression inhibited the expression of SMAD4 in HASMCs

alteration has been highlighted in several heritable connective tissue diseases with a high incidence of AD and aneurysm, including Marfan syndrome, Shprintzen-Goldberg syndrome, and Loeys-Dietz syndrome.[22] Our data showed an downregulation of SMAD4 in dissected aorta as compared with non-AD tissues. In vitro experiments were performed to further understand the association between miR146a-5p and SMAD4 in VSMCs. The results suggested that the abnormal expression of miR146a-5p could alter the expression of SMAD4 in VSMCs, corroborating a targeted regulation of SMAD4 by miR-146a-5p.

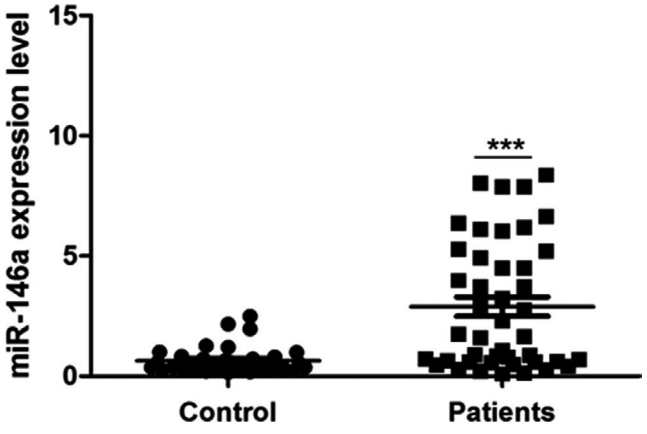

FIGURE 5 Circulating miR-146a level was significantly higher in AD patients compared with healthy controls

This study had several limitations. Firstly, our results were based on a small sample size; thus, subsequent studies should endeavor to expand AD samples, including both tissue and plasma specimens, to further confirm the results. Secondly, the association between miRNA-146a-5p and VSMCs in aortic wall degeneration needs to be further to be further elucidated, Thirdly, as a sectional study, our results confirmed elevation of circulating miR-146a-5p in the AD group, whereas the trend change of circulating miR-146a-5p level from AD onset to recovery, and further the association of circulating miR-146a-5p level with the severity of AD, remains elusive, limiting miR-146a-5p as a potential biomarker for predicting prognosis of AD.

Therefore, prospective AD cohort study, as well as further in vitro studies with VSMCs lines from dissected aorta, should be performed to address these shortcomings in the future.

In summary, this study suggested upregulation of miR146a-5p and downregulation of SMAD4 in AD tissues. The ectopic expression of miR146a-5p could promote VSMC proliferation and migration, whereas miR146a-5p negatively regulated the expression of SMAD4 by targeting the 3'-UTR of SMAD4. Therefore, the results suggested that miR146a-5p participated in the pathogenesis of AD by directly targeting SMAD4, providing new insights into effective prevention and treatment of AD.

ACKNOWLEDGMENTS

The authors thank all the participating volunteers for their efforts and contributions. This study was supported by the grants from the Science and Technology Planning Project (No. 201300000180), the National Natural Science Foundation (No. 81300230 and 81470571), the Guangdong Province Science and Technology Programme (2014A020215023), the Guangzhou City Science and Technology Programme (201508020114), and the National Key R&D Program of China (2017YFC130800).

CONFLICTS OF INTEREST

The authors declare that they have no competing interests.

ORCID

Jianfang Luo https://orcid.org/0000-0003-3220-1280

REFERENCES

1. Xue L, Luo JF, Mai JZ, Liu XQ. Change trend of clinical characteristics of aortic dissection over 10 years. *Zhonghua Xin Xue Guan Bing Za Zhi*. 2007;35:47-50.
2. Golledge J, Eagle KA. Acute aortic dissection. *Lancet*. 2008;372:55-66.
3. Barbour JR, Spinale FG, Ikonomidis JS. Proteinase systems and thoracic aortic aneurysm progression. *J Surg Res*. 2007;139:292-307.
4. Wang X, LeMaire SA, Chen L, et al. Increased collagen deposition and elevated expression of connective tissue growth factor in human thoracic aortic dissection. *Circulation*. 2006;114:I200-205.
5. Hopkins PN. Molecular biology of atherosclerosis. *Physiol Rev*. 2013;93:1317-1542.
6. Choi MH, Lee IK, Kim GW, et al. Regulation of PDGF signalling and vascular remodelling by peroxiredoxin II. *Nature*. 2005;435:347-353.
7. Testa U, Pelosi E, Castelli G, Labbaye C. miR-146 and miR- 155: two key modulators of immune response and tumor development. *Noncoding RNA*. 2017;3:E22.
8. Xiao WZ, Lu AQ, Liu XW, Li Z, Zi Y, Wang ZW. Role of miRNA-146 in proliferation and differentiation of mouse neural stem cells. *Biosci Rep*. 2015;35:e00245.
9. Katoh H, Suzuki T, Hiroi Y, et al. Diagnosis of aortic dissection by immunoassay for circulating smooth muscle myosin. *Lancet*. 1995;345:191-192.
10. Liao M, Zou S, Weng J, et al. A microRNA profile comparison between thoracic aortic dissection and normal thoracic aorta indicates the potential role of microRNAs in contributing to thoracic aortic dissection pathogenesis. *J Vasc Surg*. 2011;53(1341–1349):e1343.
11. Cordes KR, Sheehy NT, White MP, et al. miR-145 and miR-143 regulate smooth muscle cell fate and plasticity. *Nature*. 2009;460:705-710.
12. Cheng Y, Liu X, Yang J, et al. MicroRNA-145, a novel smooth muscle cell phenotypic marker and modulator, controls vascular neointimal lesion formation. *Circ Res*. 2009;105:158-166.
13. Elia L, Quintavalle M, Zhang J, et al. The knockout of miR-143 and -145 alters smooth muscle cell maintenance and vascular homeostasis in mice: correlates with human disease. *Cell Death Differ*. 2009;16:1590-1598.
14. Hu ZY, Luo JF, Zhong SL, Xue L, Chen YF, Fan RX. MicroRNAs expression in normal and dissected aortic tissue. *Zhonghua Xin Xue Guan Bing Za Zhi*. 2012;40:406-410.
15. Suzuki T, Katoh H, Watanabe M, et al. Novel biochemical diagnostic method for aortic dissection. Results of a prospective study using an immunoassay of smooth muscle myosin heavy chain. *Circulation*. 1996;93:1244-1249.
16. Zhu L, Vranckx R, Khau Van Kien P, et al. Mutations in myosin heavy chain 11 cause a syndrome associating thoracic aortic aneurysm/aortic dissection and patent ductus arteriosus. *Nat Genet*. 2006;38:343-349.
17. Satoh K, Matoba T, Suzuki J, et al. Cyclophilin A mediates vascular remodeling by promoting inflammation and vascular smooth muscle cell proliferation. *Circulation*. 2008;117:3088-3098.
18. Muller BT, Modlich O, Prisack HB, et al. Gene expression profiles in the acutely dissected human aorta. *Eur J Vasc Endovasc Surg*. 2002;24:356-364.
19. Wang L, Zhang J, Fu W, Guo D, Jiang J, Wang Y. Association of smooth muscle cell phenotypes with extracellular matrix disorders in thoracic aortic dissection. *J Vasc Surg*. 2012;56(1698–1709):1709.e1691.
20. Zhang X, Cao J, Pei Y, Zhang J, Wang Q. Smad4 inhibits cell migration via suppression of JNK activity in human pancreatic carcinoma PANC-1 cells. *Oncol Lett*. 2016;11:3465-3470.
21. Chu P, Liang A, Jiang A, Zong L. miR-205 regulates the proliferation and invasion of ovarian cancer cells via suppressing PTEN/SMAD4 expression. *Oncol Lett*. 2018;15:7571-7578.
22. Doyle AJ, Doyle JJ, Bessling SL, et al. Mutations in the TGF-beta repressor SKI cause Shprintzen-Goldberg syndrome with aortic aneurysm. *Nat Genet*. 2012;44:1249-1254.

SUPPORTING INFORMATION

Additional supporting information may be found online in the Supporting Information section at the end of the article.

How to cite this article: Xue L, Luo S, Ding H, et al. Upregulation of miR-146a-5p is associated with increased proliferation and migration of vascular smooth muscle cells in aortic dissection. *J Clin Lab Anal*. 2019;33:e22843. https://doi.org/10.1002/jcla.22843